RESEARCH ARTICLE

Key Points:
- A *Pyrosoma atlanticum* swarm was observed in a cold-core eddy of the Tasman Sea where there was an increased proportion of favorable food
- The *P. atlanticum* population feeding at the surface consumed 95% of the local phytoplankton standing stock in one night
- Total downward carbon flux produced by the migrating *P. atlanticum* swarm was 11 mg C·m^{-2}·d^{-1}

Large Vertical Migrations of *Pyrosoma atlanticum* Play an Important Role in Active Carbon Transport

Natasha Henschke[1] (iD), Evgeny A. Pakhomov[1,2,3], Lian E. Kwong[1], Jason D. Everett[4,5] (iD), Leonardo Laiolo[6,7], Amy R. Coghlan[8], and Iain M. Suthers[4,5] (iD)

[1]Department of Earth, Ocean and Atmospheric Sciences, University of British Columbia, Vancouver, British Columbia, Canada, [2]Institute for the Oceans and Fisheries, University of British Columbia, Vancouver, British Columbia, Canada, [3]Hakai Institute, Heriot Bay, British Columbia, Canada, [4]Evolution and Ecology Research Centre, University of New South Wales, Sydney, New South Wales, Australia, [5]Sydney Institute of Marine Science, Mosman, New South Wales, Australia, [6]Climate Change Cluster, University of Technology Sydney, Ultimo, New South Wales, Australia, [7]CSIRO Oceans and Atmosphere, Hobart, Tasmania, Australia, [8]Institute for Marine and Antarctic Studies, University of Tasmania, Hobart, Tasmania, Australia

Abstract Pyrosomes are efficient grazers that can form dense aggregations. Their clearance rates are among the highest of any zooplankton grazer, and they can rapidly repackage what they consume into thousands of fecal pellets per hour. In recent years, pyrosome swarms have been found outside of their natural geographical range; however, environmental drivers that promote these swarms are still unknown. During the austral spring of 2017 a *Pyrosoma atlanticum* swarm was sampled in the Tasman Sea. Depth-stratified sampling during the day and night was used to examine the spatial and vertical distribution of *P. atlanticum* across three eddies. Respiration rate experiments were performed onboard to determine minimum feeding requirements for the pyrosome population. *P. atlanticum* was 2 orders of magnitude more abundant in the cold core eddy (CCE) compared to both warm core eddies, with maximum biomass of 360 mg WW·m^{-3}, most likely driven by high chlorophyll *a* concentrations. *P. atlanticum* exhibited diel vertical migration and migrated to a maximum depth strata of 800–1,000 m. Active carbon transport in the CCE was 4 orders of magnitude higher than the warm core eddies. Fecal pellet production contributed to the majority (91%) of transport, and total downward carbon flux below the mixed layer was estimated at 11 mg C·m^{-2}·d^{-1}. When abundant, *P. atlanticum* swarms have the potential to play a major role in active carbon transport, comparable to fluxes for zooplankton and micronekton communities.

Plain Language Summary Pyrosomes are a gelatinous zooplankton that can form large swarms. They feed through filtration and are among the most efficient filter feeders of any zooplankton, repackaging what they consume into thousands of fecal pellets per hour. As pyrosomes migrate vertically to 800 m daily, they have the potential to transport the carbon they consume at the surface to these depths. In the austral spring of 2017 we sampled a pyrosome swarm in the Tasman Sea. Maximum biomass of pyrosomes was 360 mg WW·m^{-3}, and pyrosomes were able to consume the majority (95%) of the phytoplankton community while at the surface. When migrating below the surface, they transported 11 mg C·m^{-2}·d^{-1} below the mixed layer, mostly through fecal pellets (91%). This flux is within the range of fluxes produced by zooplankton and micronekton communities.

1. Introduction

Pyrosomes are colonial pelagic tunicates comprised of thousands of individual zooids that form a hollow, gelatinous cylinder that is closed at one end (Godeaux et al., 1998). They can grow up to 20 m in length and are found in the epipelagic and mesopelagic layers of warm oceans between 50°N and 50°S (van Soest, 1981). Although they can form dense aggregations (e.g., Andersen & Sardou, 1994; Brodeur et al., 2018; Drits et al., 1992), the trophic function and ecology of pyrosomes are not well known and they are the least studied of all pelagic tunicates (Henschke et al., 2016; Madin & Deibel, 1998).

Pyrosoma atlanticum is the most abundant pyrosome in the Pacific Ocean, found at temperatures from 7 to 30 °C, and normally ranging in size from less than 1 to 60 cm (Thompson, 1948). Pyrosomes are filter feeders, with each zooid filtering water from the outside of the colony through a ciliated branchial basket where food is captured on mucous sheets, before being expelled into the hollow cavity of the colony (Madin & Deibel,

1998). The feeding momentum by each zooid makes pyrosomes the only animal that uses continuous jet propulsion, allowing them to move slowly forward while continuously grazing (Bone, 1998). As a result, pyrosomes are efficient feeders, with *P. atlanticum* having among the highest clearance rates of any zooplankton grazer, up to 35 L h^{-1} (Perissinotto et al., 2007). They also rapidly produce fecal pellets, with each zooid producing two fecal pellets per hour (Drits et al., 1992). Considering there can be thousands of zooids in a colony, this equates to one 60 mm colony producing the same amount of fecal pellets as approximately 500 *Calanus* copepods (Drits et al., 1992).

Similar to other pelagic tunicates such as salps, pyrosomes are an important prey item in the diet of many pelagic and benthic animals (Henschke et al., 2016) and have a relatively high carbon content for a gelatinous organism (35% DW; Lebrato & Jones, 2009). In the pelagic environment, pyrosomes are consumed by 62 fish species, sea birds, turtles, and sea lions (Childerhouse et al., 2001; Harbison, 1998; Hedd & Gales, 2001). When they migrate to the sea floor, either by sinking rapidly after death (Lebrato & Jones, 2009) or through daily vertical migrations up to 900 m depth (Andersen et al., 1992; Andersen & Sardou, 1994; Angel, 1989; Roe et al., 1987), pyrosomes are known to be consumed by 33 species of benthic organisms including sea anemones, sea urchins and crabs at depths of up to 2102 m (Archer et al., 2018). The transfer of pyrosome carcasses to depth within the ocean can provide a substantial (and accelerated) input of carbon, up to 13 times greater than the average annual flux (Lebrato & Jones, 2009). Therefore, they are expected to play an important role in the vertical transport of carbon in the ocean, either through predation, carcass deposition or fecal pellet production.

Environmental drivers that promote pyrosome swarms are still unknown, despite dense aggregations being found in the southwest Pacific (Thompson, 1948), California Current (Berner, 1967), Mediterranean Sea (Andersen & Sardou, 1994), the Atlantic Ocean (Drits et al., 1992), the Gulf of Mexico (Archer et al., 2018), and most recently in the northeast Pacific (Brodeur et al., 2018; Sutherland et al., 2018). These aggregations can reach up to 40 colonies m^{-3} (Drits et al., 1992) or 200 mg WW·m^{-3} (Brodeur et al., 2018). Considering their high clearance rates, fecal pellet production, diel vertical migration (DVM) and contribution to the benthos at the demise of the swarm, such large aggregations are likely to play a major role in marine ecosystems, and potentially accelerate the vertical transport of carbon.

During the austral spring of 2017, a dense *Pyrosoma atlanticum* swarm was observed within adjacent eddies of the southwest Pacific. This enabled an investigation into factors influencing the distribution, abundance and trophic impact of pyrosomes on the local ecosystem. In particular, this study aimed to (a) examine the spatial and vertical structure of *P. atlanticum* populations across three eddies, (b) determine the energetic requirements of a *P. atlanticum* swarm by calculating their respiration rate, and (c) quantify the contribution of a *P. atlanticum* swarm to the local vertical carbon flux.

2. Methods

2.1. Oceanographic Sampling Procedure

Pyrosome and micronekton (20–100 mm; Brodeur et al., 2004) sampling was undertaken onboard the RV *Investigator* in the Tasman Sea from 6 to 15 September 2017. The western Tasman Sea is characterized by frequent cyclonic and anticyclonic eddies (Everett et al., 2012), forming as the East Australian Current (EAC) diverges eastward from the Australian shelf (Suthers et al., 2011). Although temporally and spatially patchy, cyclonic (generally upwelling) and anticyclonic (generally downwelling) eddies greatly contribute to the mixing of the upper ocean in this region (Tilburg et al., 2002). The presence of eddies in the western Tasman Sea results in a patchwork of pelagic habitats, with anticyclonic eddies tending to be less productive than the more enriched cyclonic eddies (Everett et al., 2012). The sampling area extended from Newcastle (33°S) southward to Batemans Bay (35.7°S; Figure 1). Three eddies were identified during the voyage using a combination of satellite-derived sea-surface temperature, chlorophyll *a* (from Moderate Resolution Imaging Spectroradiometer; MODIS-Aqua) and altimetry data which was extracted from the Integrated Marine Observing System Data Portal (http://imos.aodn.org.au/imos/). The three eddies were an anticyclonic warm core eddy that formed from the retroflection of the EAC (R-WCE), and two eddies that were closely adjacent (an eddy dipole) sampled south of the Tasman Front. The eddy dipole consisted of a cyclonic cold core eddy (CCE) and an anticyclonic warm core eddy (WCE).
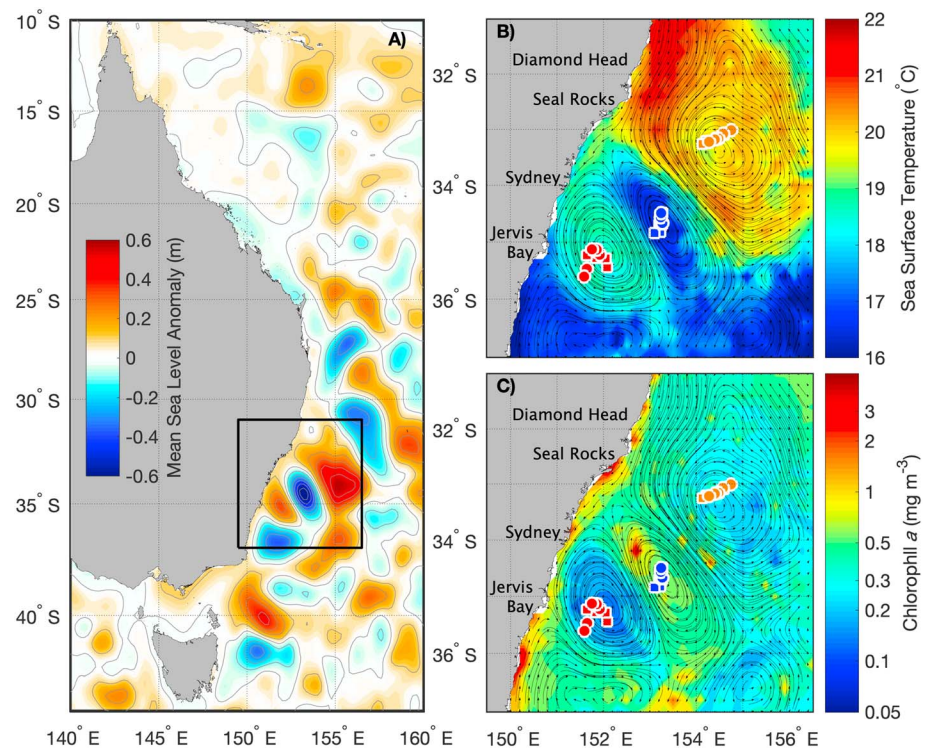
Figure 1. Location plot with satellite-derived (a) mean sea level anomaly (m), (b) sea surface temperature (°C), and (c) chlorophyll a concentration (mg m^{-3}). Arrows in (b) and (c) represent geostrophic currents estimated through surface altimetry. Shapes represent CTD (squares) and trawl (circles) sampling locations at the R-WCE (orange), CCE (blue), and WCE (red). Surface altimetry data are the midpoint of sampling (9 September 2017) and was obtained from IMOS. Sea surface temperature and chlorophyll a concentration plots are representative of the voyage (mean of 31 August to 18 September 2017) and was obtained from MODIS-Aqua. CTD = conductivity-temperature-depth; R-WCE = anti-cyclonic warm core eddy that formed from the retroflection of the East Australian Current; CCE = cold core eddy; WCE = warm core eddy; MODIS = Moderate Resolution Imaging Spectroradiometer.

At transects along each eddy, a Seabird SBE911-plus conductivity-temperature-depth (CTD) probe equipped with a calibrated Chelsea Aqua-Tracker Mk3 fluorometer was used to profile salinity, temperature, and fluorescence. CTD fluorometer readings were converted to chlorophyll a concentrations by calculating a linear fit between CTD fluorometer readings and CTD Niskin bottle samples ($n = 20$, $R^2 = 0.84$). Specifically, surface water (i.e., 5 to 10 m depth) was sampled from the CTD-rosette and transferred into acid-cleaned 2 L polycarbonate vessels. Directly on board, 250 mL of water per sample was then filtered parallel through two independent filters: a 25 mm glass fiber filter with nominal pore size of 0.3 μm (Sterlitech, USA) and a 25 mm polycarbonate membrane with pore size of 10 μm (Merck Millipore, USA). Filters were then transferred into cryotubes, flash frozen in liquid nitrogen and then stored in a −80 °C freezer. Each filter was then placed into an individual 15 mL centrifuge tube containing 2 mL of 90% acetone. Pigments were extracted at 4 °C overnight in the dark. Chlorophyll a concentrations were determined using a calibrated fluorometer (Chlorophyll a Non Acidified module; Trilogy, Turner Design, USA). While we assumed the chlorophyll a concentration determined from the 0.3 μm filter represented total chlorophyll a, the chlorophyll a associated with phytoplankton >10 μm was determined by the 10 μm filters.

From the surface water sampled from the CTD-rosette another 200 mL were collected in brown glass bottles, then fixed with 2% Lugol's iodine and stored under cool (i.e., 4 °C) and dark conditions for subsequent Coulter Counter analyses, performed at the Ocean and Atmosphere laboratories at Hobart CSIRO (The Commonwealth Scientific and Industrial Research Organisation). The phytoplankton carbon content was then estimated based on the measured volume from the Coulter Counter analyses and volume to carbon conversion from Montagnes et al. (1994).

Depth-stratified sampling for pyrosomes and micronekon was undertaken along each transect using an International Young Gadoid Pelagic trawl equipped with a MIDwater Open and Closing net system

(MIDOC; Marouchos et al., 2017). Mesh size of the trawl reduced from 200 mm stretched mesh width at the mouth to 10 mm in the codend. Within the MIDOC, the six codends graduated from 10 mm mesh to 500 μm mesh where the microneketon was collected. Trawls were performed at day and night while the vessel maintained a speed of 1 m s^{-1}. Samples were taken obliquely from 1,000–800 m, then at 100 m depth intervals from 800 m to the surface, with each net fishing for approximately 20 min. Additional samples were taken in the top 100 m using a Danish trawl (300 μm mesh) without a MIDOC that was towed at 1 m s^{-1} obliquely for 60 min. Immediately after collection, pyrosomes and micronekton were separated into major taxonomic groups, weighed and measured for body length (mm). The major taxonomic groups were: fish, crustaceans, molluscs, jellyfish, pelagic tunicates, and worms.

2.2. Shipboard Respiration Experiments

Respiration experiments for *Pyrosoma atlanticum* were undertaken with live individuals obtained from surface trawls in the CCE. Individuals were transferred into 2.4 L polyethylene containers with natural seawater ($n = 13$). Containers were carefully filled to the surface before sealing to prevent the introduction of oxygen from the air. Controls containing no pyrosomes were also prepared ($n = 3$). Experiments ran for 4 hours at 17 °C. Dissolved oxygen concentrations at the end of the experiments were determined using the Winkler-titration method (Strickland & Parsons, 1972). After the experiment, lengths and wet weights of the pyrosomes were measured. To compare respiration measurements against other studies, measurements were corrected for temperature as per Gillooly et al. (2001).

2.3. Clearance Rates and Population Minimum Food Requirements

Pyrosoma atlanticum clearance rates (*CR*; L·colony^{-1}·h^{-1}) can be expressed as a function of length using empirical data from Perissinotto et al. (2007) and Drits et al. (1992):

$$CR = 0.0558l^{1.174} \quad \left(n = 9, R^2 = 0.59\right) \tag{1}$$

where l is colony length (mm).

Population minimum food requirement (PMFR, mg C·m^{-3}·d^{-1}) can be estimated from respiration rates using the following empirical formula (Uye & Shimauchi, 2005):

$$PMFR = \frac{RC \cdot B}{A \cdot W} \tag{2}$$

where RC is the respiratory carbon equivalent (RC; μg C·colony^{-1}·h^{-1}; see equation (4)), B is the biomass of pyrosomes (g WW·m^{-3}), A is the assimilation efficiency (0.64; Iguchi & Ikeda, 2004) and W is the average wet weight (g). As there is no A value for pyrosomes, here we assume the value for salps, a close relative, will be representative.

2.4. Active Carbon Transport

The *Pyrosoma atlanticum* migratory community was calculated based on the day and night difference in *P. atlanticum* biomass within the mixed layer. This method corrects for daytime surface residents; hence, only the portion of vertically migrating *P. atlanticum* were included in our calculation of active carbon flux for each water mass.

To determine the migratory depth of *Pyrosoma atlanticum* the weighted mean depth (WMD, m) was calculated:

$$WMD = \frac{\sum (b_i \cdot d_i)}{\sum b_i} \tag{3}$$

where b_i is the biomass of pyrosomes (mg WW·m^{-3}) and d_i is the midpoint of the depth stratum in each sampling location i.

To calculate the contribution of *Pyrosoma atlanticum* to active carbon transport, we must first calculate respiration, excretion, gut flux (defecation), and mortality. For respiration, excretion and gut flux (defecation) we apply size-dependent rate equations.

Size-based respiratory rates of oxygen uptake (ml O$_2$·colony^{-1}·d^{-1}) were estimated using shipboard experiments. As these experiments were conducted at 17 °C, we use Q$_{10}$ = 2.8 (Iguchi & Ikeda, 2004) to correct for

Table 1
Hours Spent at Day and Night Depths, and During Vertical Migration (Between Surface and Depth), Derived From EK60

	Upward migration (h)	Surface (h)	Downward migration (h)	Depth (h)
R-WCE	1	11.5	1.5	10
CCE	2	12	1	9
WCE	2.5	11	1	9.5

differences in temperature between depth strata. To calculate respiratory carbon equivalent (RC; μg C·colony^{-1}·d^{-1}) we apply the following equation from Al-Mutairi and Landry (2001):

$$RC = R \cdot RQ \cdot \left(\frac{12}{22.4} \right) \tag{4}$$

where R is the respiration rate (ml O$_2$·colony^{-1}·d^{-1}; see equation (8)), RQ is the respiratory quotient (1.16; Mayzaud et al., 2005), 12 is the molar weight of carbon (g mol^{-1}), and 22.4 is the molar volume (mol L^{-1}) of an ideal gas at standard pressure and temperature. As there is no RQ value for pyrosomes, here we assume that the value for salps will be representative. To calculate depth specific respiration (μg·C m^{-3}·h^{-1}) for each size class, we multiply R by abundance and time spent at each depth.

There are no known estimates for excretion rates and mortality of *Pyrosoma atlanticum*. Dissolved organic carbon (DOC) excretion was assumed to be approximately equivalent to 31% of the C respired (RC) and was determined using estimates for macrozooplankton and micronekton in Steinberg et al. (2000). Mortality rates for *P. atlanticum* are assumed to be comparable to that of a similar sized salp (4–150 mm), *Salpa thompsoni* (Henschke et al., 2018). Mortality ranged from 1% d^{-1} in areas with low biomass (RWCE and WCE) to 5% d^{-1} in areas with high biomass (CCE), based on the assumption that the biomass of predators scales with the biomass of prey (Steele & Henderson, 1993).

To estimate gut flux (total nondigested food or defecation), we first calculate daily fecal pellet production (FP; mg C·colony^{-1}·d^{-1}) based on colony carbon weight (CW; mg C; Drits et al., 1992):

$$FP = 0.25 \cdot CW \tag{5}$$

such that daily defecation rates are 25% of body carbon, which is consistent with values previously identified for salps (10–30% body C d^{-1}; Madin & Deibel, 1998). Carbon weight is estimated to be 3.92% of wet weight (Lebrato & Jones, 2009). Here, we assume that FP is constant throughout the day as *Pyrosoma atlanticum* is continually feeding. We applied a gut passage time (GPT; h) of 1.43 (Perissinotto et al., 2007), and used time spent migrating (Table 1) to calculate the portion of nondigested food from the surface being transported to each depth strata during downward vertical migration. Hence, the daily gut flux transported to depth by each colony (GF; mg C·colony^{-1}·d^{-1}) is

$$GF = \frac{FP}{24} \cdot (GPT - DM) \tag{6}$$

where 24 converts daily FP to hourly. DM is the time spent on downward migration (h), and must not exceed GPT. For example, in the R-WCE the time spent migrating exceeded gut passage time so nondigested food consumed at the surface would have been eliminated during downward migration. Time spent at depth, migrating, and at the surface were estimated based on the rate of ascent from the deep scattering layer using acoustic backscatter from the onboard EK60 (Suthers, 2017), and swimming speeds in this study (0.03–0.07 m s^{-1}) were within the range observed for salps (0.02–0.14 m s^{-1}; Sutherland & Madin, 2010).

2.5. Data Analysis

An analysis of variance was conducted to compare environmental conditions between water types and to compare *Pyrosoma atlanticum* biomass and size distribution across locations, depth, and sampling time. A nonlinear generalized additive mixed-effects model ("mgcv" package in *R*; Wood, 2006) was used to examine the environmental drivers of *P. atlanticum* biomass, with temperature and chlorophyll *a* included as explanatory variables. The most parsimonious model was chosen by comparing Akaike's information criterion across models.

Table 2
Mean Characteristics (±SD) Over the Top 100 m of the Water Column. The Mixed Layer Depth Is Calculated From the Minimum Depth to Which T < T(10 m) − 0.4 °C Following Condie and Dunn (2006)

Water type	n	Mixed layer depth (m)	Temperature (°C)	Salinity	Chlorophyll a (mg m^{-3})	C:Chl (gr gr^{-1})
R-WCE	6 (2)	226 ± 72.3*	19.96 ± 0.11*	35.77 ± 0.01*	0.45 ± 0.06*	17.13 ± 4.74*
CCE	8 (3)	185.8 ± 11.3*	15.99 ± 0.07**	35.58 ± 0.01**	1.33 ± 0.22**	37.72 ± 2.16**
WCE	10 (3)	308.6 ± 31.2**	18.55 ± 0.06***	35.77 ± 0.01*	0.43 ± 0.14*	20.42 ± 4.14*

Note. n = number of stations. Numbers in brackets denote number of stations for C:Chl estimation.
*,**,***Significant differences at *p* < 0.01.

3. Results

3.1. Oceanographic Conditions

During sampling, the EAC separated from the coast at 33°S and a large 200 km anticyclonic (warm core) eddy formed from the main retroflection of the EAC (R-WCE; Figure 1). The R-WCE was deeply mixed (226 ± 72.3 m) and was characterized by warm (19.96 ± 0.11 °C), low chlorophyll *a* water (0.45 ± 0.06 mg m^{-3}; Table 2 and Figure 2). South of the Tasman Front was an eddy dipole composed of a northern cyclonic cold-core eddy (CCE) and a southern anticyclonic warm core eddy (WCE; Figure 1). Similar to the R-WCE, satellite observations show that the WCE was formed from EAC water, whereas the CCE was formed from Tasman Sea water. Both the CCE (185.8 ± 11.3 m) and the WCE (308.6 ± 31.2 m) had deep mixed layers; however, the CCE was characterized by significantly cooler water (15.99 ± 0.07 °C; $F_{2,23}$ = 4751.62, *p* < 0.001), and significantly higher chlorophyll *a* concentrations (1.33 ± 0.22 mg m^{-3}; $F_{2,23}$ = 81.24, *p* < 0.001; Table 2). Size-fractionated chlorophyll *a* analyses indicated that the CCE had higher proportions (54%) of larger phytoplankton (>10 μm) compared to the WCE (1%) and the R-WCE (3%; Figure 3a). Carbon
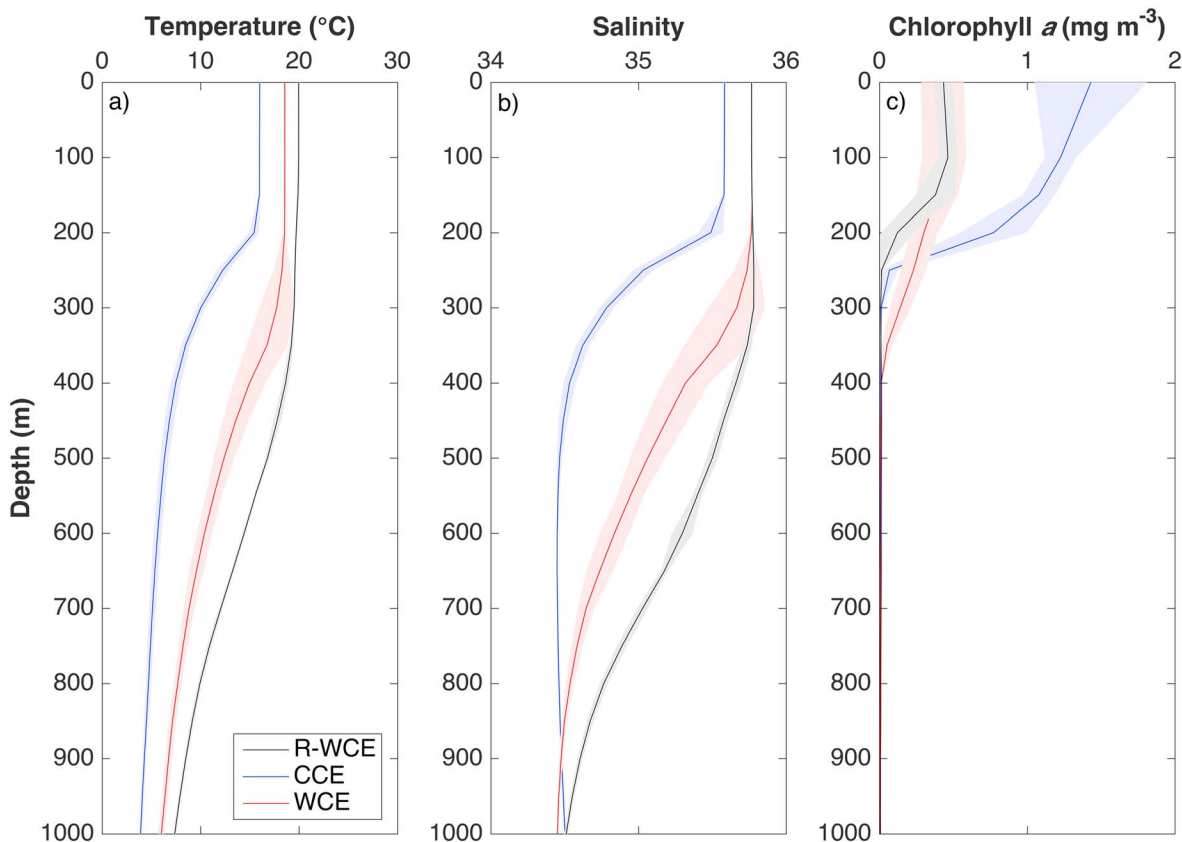

Figure 2. Depth profiles of (a) temperature (°C), (b) salinity, and (c) chlorophyll *a* (mg m^{-3}) in the R-WCE (black), CCE (blue), and WCE (red). Shaded values indicate standard deviation around the mean. R-WCE = anti-cyclonic warm core eddy that formed from the retroflection of the East Australian Current; CCE = cold core eddy; WCE = warm core eddy.

Figure 3. Mean (±SD) log biomass of (a) total chlorophyll *a* (black bars) and phytoplankton >10 μm (gray bars) and (b) *Pyrosoma atlanticum* (black bars) and all other micronekton (gray bars) at the R-WCE, CCE, and WCE. R-WCE = anti-cyclonic warm core eddy that formed from the retroflection of the East Australian Current; CCE = cold core eddy; WCE = warm core eddy.
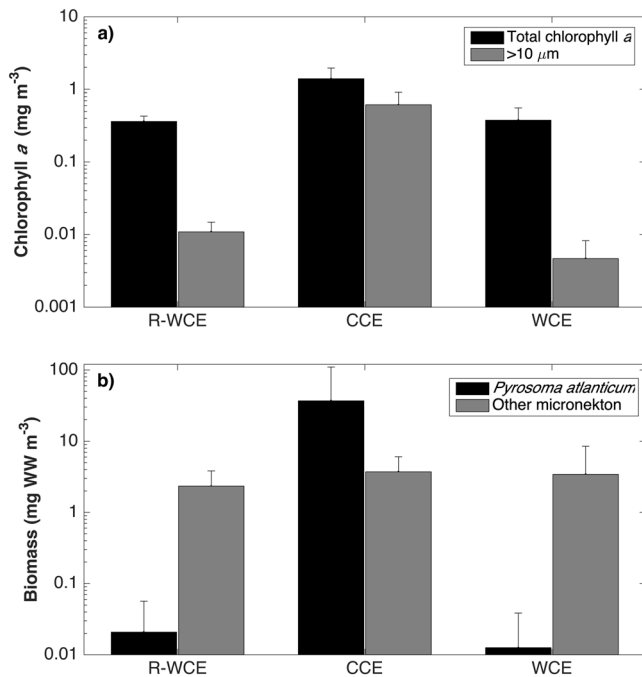
to chlorophyll *a* ratios (C:Chl, g g^{-1}) were significantly higher in the CCE (37.72) compared to the WCE (20.42) and the R-WCE (17.13; $F_{2,7} = 25.09$, $p = 0.0025$; Table 2).

3.2. *Pyrosoma atlanticum* Spatial Distribution

Total depth-integrated *Pyrosoma atlanticum* biomass was significantly higher in the CCE (36.83 ± 73.43 mg WW·m^{-3}; range: 0.26–360.44) compared to the R-WCE (0.02 ± 0.04 mg WW·m^{-3}; range: 0.003–0.13) and the WCE (0.01 ± 0.03 mg WW·m^{-3}; range: 0.003–0.14; $F_{2,97} = 8.98$, $p < 0.001$; Figure 3b). Correspondingly, *P. atlanticum* abundance was significantly higher in the CCE (2.85 ± 4.74 indviduals (ind.) 1,000 m^{-3}) compared to the R-WCE (0.08 ± 0.09 ind. 1,000 m^{-3}) and the WCE (0.08 ± 0.14 ind. 1,000 m^{-3}; $F_{2,39} = 5.26$, $p < 0.01$). There was no significant difference in depth-integrated pyrosome biomass between day and night across water types.

Micronekton (excluding pyrosome) biomass (±SD) did not differ between eddies, ranging from 2.34 ± 1.50 mg WW·m^{-3} in the R-WCE to 3.43 ± 5.10 mg WW·m^{-3} in the WCE and 3.73 ± 2.34 mg WW·m^{-3} in the CCE (Figure 3b). Pyrosomes made up the majority of total micronekton biomass in the CCE (91%) compared to the warm core eddies where they only comprised <1% of total micronekton biomass. Micronekton (excluding pyrosome) biomass was dominated by fish in the R-WCE (68%) and the CCE (70%) and by molluscs (mainly squid) in the WCE (34%).

The most parsimonious model explaining variations in *P. atlanticum* biomass across all sampling sites only included chlorophyll *a* as a driver, with *P. atlanticum* biomass increasing significantly with increasing chlorophyll *a* concentrations ($edf = 1.983$, $F = 10.2$, $p < 0.001$).

3.3. *Pyrosoma atlanticum* Size Distribution

Pyrosoma atlanticum colonies were significantly smaller in the R-WCE and the WCE compared to the CCE ($F_{2,709} = 632.32$, $p < 0.001$). In the R-WCE, colonies ranged from 4.05 to 77.44 mm, with an average size of 13.39 mm (Figure 4a). Similarly, colonies in the WCE ranged from 3.61 to 37.65 mm long, with an average size of 11.16 mm (Figure 4b). In the CCE, colonies were much larger, on average 107.92 mm long and ranging in size from 11.22 to 317.62 mm (Figure 4c). 92% of colonies in the CCE were of reproductive size (> 40 mm; van Soest, 1981), compared to 5% in the R-WCE, and none in the WCE. Colony size distribution did not vary significantly with depth.

3.4. *Pyrosoma atlanticum* Respiration

Pyrosoma atlanticum wet weight increased with length (Figure 5a) as expressed by:

$$WW = 0.0013l^2 + 0.0151l \qquad (n = 192, R^2 = 0.90) \tag{7}$$

where WW is wet weight (g) and *l* is colony length (mm).

At 17 °C, the respiration rates of *P. atlanticum* (wet weight: 5.5–43 g) were expressed by the following allometric equation (Figure 5b):

$$R = 0.0046WW^{1.2284} \qquad (n = 13, R^2 = 0.95) \tag{8}$$

where *R* is the respiration rate (ml O$_2$·colony^{-1}·h^{-1}) and WW is the wet weight of the pyrosome colony (g).

3.5. *Pyrosoma atlanticum* Vertical Distribution

The average weighted mean depth (WMD) of the *P. atlanticum* population during the day (343.33 ± 147.92 m) was lower than during the night (120.96 ± 66.21 m), suggesting that individuals in all three water masses were undergoing diel vertical migrations. We were unable to statistically test the
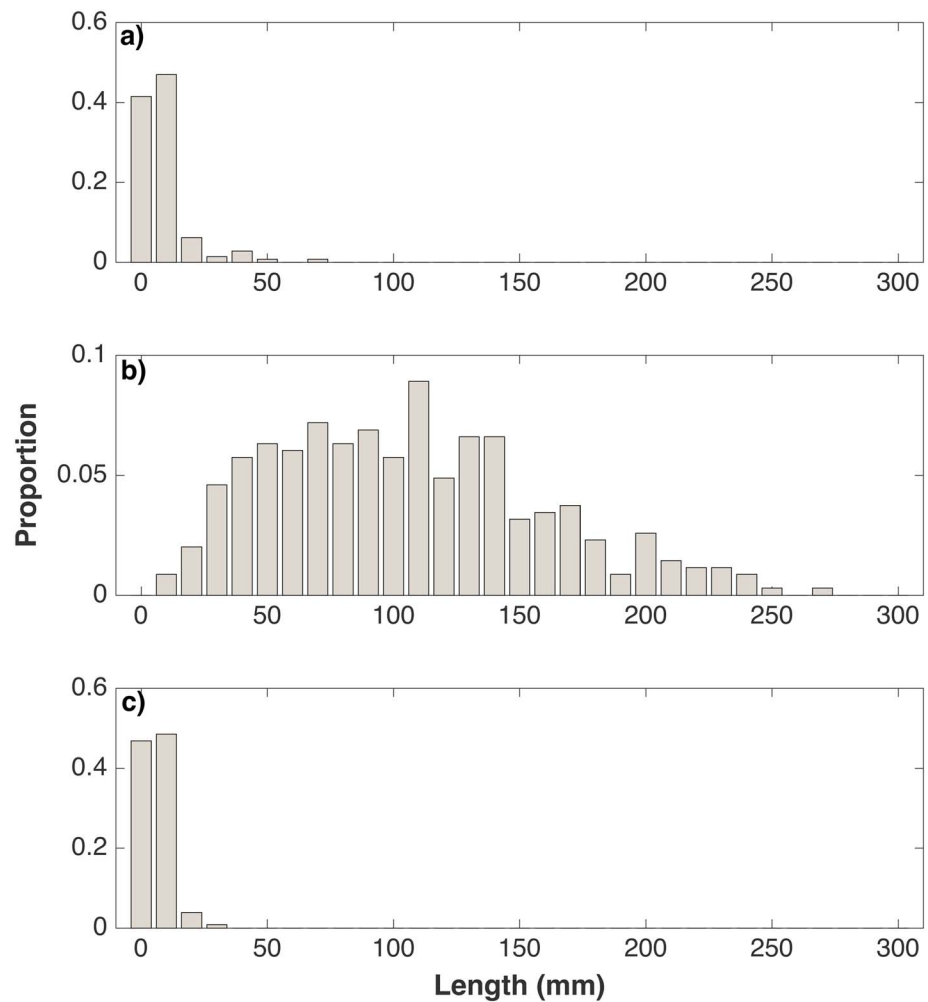
Figure 4. *Pyrosoma atlanticum* size distribution in the (a) R-WCE, (b) CCE, and (c) WCE. R-WCE = anti-cyclonic warm core eddy that formed from the retroflection of the East Australian Current; CCE = cold core eddy; WCE = warm core eddy.

differences in WMD during the day and night across water masses due to limited replication ($n = 6$). During the day, WMD (i.e., depth of carbon export) was deeper in the WCE (487 m), followed by the R-WCE (351 m) and CCE (192 m; Figure 6). At night, the WMD was shallower in the CCE (68 m) followed by the R-WCE (100 m) and the WCE (195 m), yet across all eddies the nighttime WMD coincided with the local chlorophyll *a* maxima (Figure 6). *P. atlanticum* migrated twofold further in the R-WCE (292 m) and the WCE (251 m) than in the CCE (123 m) and went below the mixed layer depth in the R-WCE and the WCE (Figure 6). In the CCE, the vertical distribution of daytime pyrosome biomass was bimodal; the WMD of the population was at the base of the mixed layer during the day; however, 30% of total biomass migrated below the mixed layer (300–500 m). Sampling was only undertaken in the top 500 m in the R-WCE and CCE, whereas in the WCE trawls were undertaken to 1,000 m. In the WCE, 42% of the pyrosome population migrated below 500 m at night, and none occurred below 500 m during the day.

3.6. Consumption, Minimum Food Requirements, and Active Carbon Transport

Consumption and minimum food requirements were estimated for *Pyrosoma atlanticum* populations in the CCE assuming a representative nighttime feeding (12 h; Table 1) population of *P. atlanticum* with biomass of 325.17 mg WW·m^{-3}. Based on a mean colony length of 107.92 mm, individual clearance rates were 13.6 L h^{-1} and individual respiration rates were 0.07 mg C·h^{-1}. Given a local phytoplankton carbon biomass of 50.17 mg C·m^{-3} (assuming C:Chl = 37.72; Table 2), the CCE pyrosome population can potentially clear 47.51 mg C·m^{-3} while feeding at the surface, 95% of the available phytoplankton carbon biomass
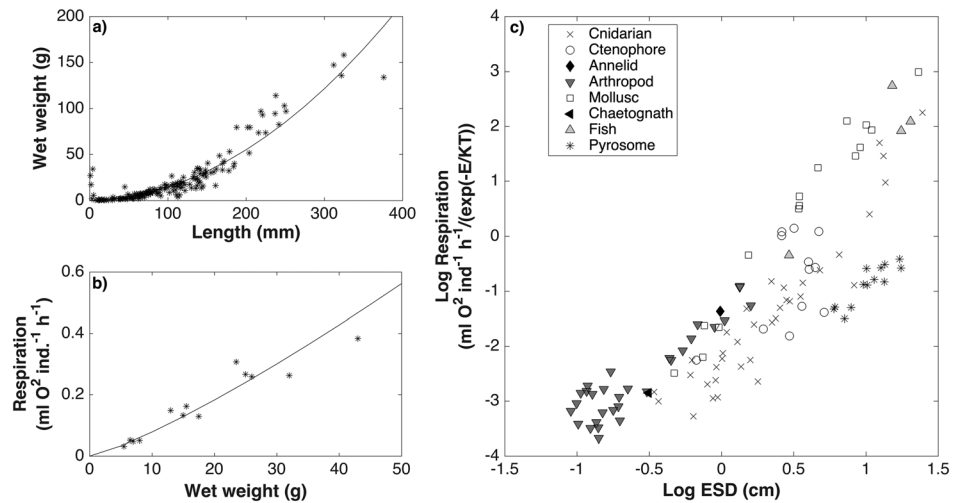
Figure 5. (a) Relationship between length and wet weight for *Pyrosoma atlanticum* showing data points (asterisks) and line of best fit ($R^2 = 0.9$). (b) Relationship between respiration rate and wet weight for *P. atlanticum* at 17 °C showing data points (asterisks) and line of best fit ($R^2 = 0.95$). (c) Respiration rate as a function of animal size (equivalent spherical diameter; ESD) for *P. atlanticum* and other pelagic animals. Data sources for animals other than *P. atlanticum* are from Pitt et al. (2013).

(Figure 7). However, they have an estimated minimum food requirement (MFR) of only 11.26 mg C·m^{-3} (22% of phytoplankton carbon biomass) to meet metabolic needs. In comparison, we estimate that in the R-WCE (0.12 mg WW·m^{-3}, 13.39 mm) and the WCE (0.31 mg WW·m^{-3}, 11.16 mm), the *P. atlanticum* populations were only consuming 0.01% (0.94 μg C·m^{-3}·d^{-1}; MFR = 0.09 μg C·m^{-3}·d^{-1}) and 0.05% (4.18 μg C·m^{-3}·d^{-1}; MFR = 0.46 μg C·m^{-3}·d^{-1}) of the phytoplankton carbon biomass while at the surface respectively.

Total downward active carbon flux varied substantially across water types (Table 3 and Figure 7). It should be noted that we were unable to test these differences statistically due to a lack of replication. Overall, total
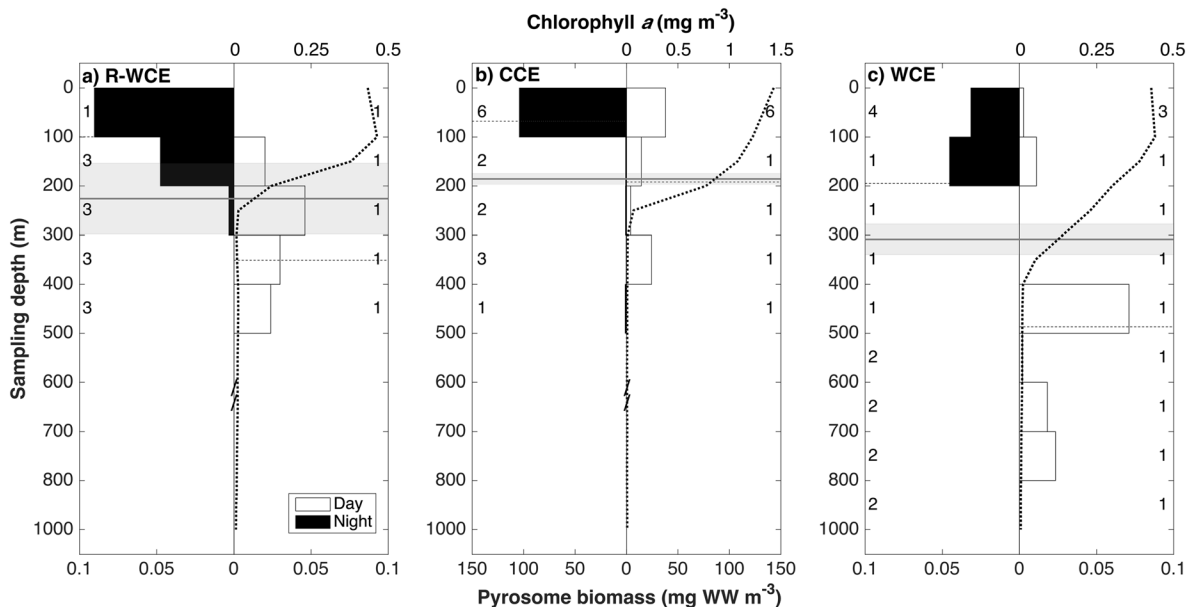

Figure 6. Depth profile of mean *Pyrosoma atlanticum* biomass (mg WW·m^{-3}) during the day (white bars) and night (black bars) at the (a) R-WCE, (b) CCE, and (c) WCE with chlorophyll *a* (mg m^{-3}) overlaid (dotted lines). Note sampling was restricted to the top 500 m in a and b. Dashed lines represent weighted mean depth. Gray lines and shaded areas represents mean (±SD) mixed layer depth. Numbers represent number of trawls performed at each depth interval. R-WCE = anti-cyclonic warm core eddy that formed from the retroflection of the East Australian Current; CCE = cold core eddy; WCE = warm core eddy.
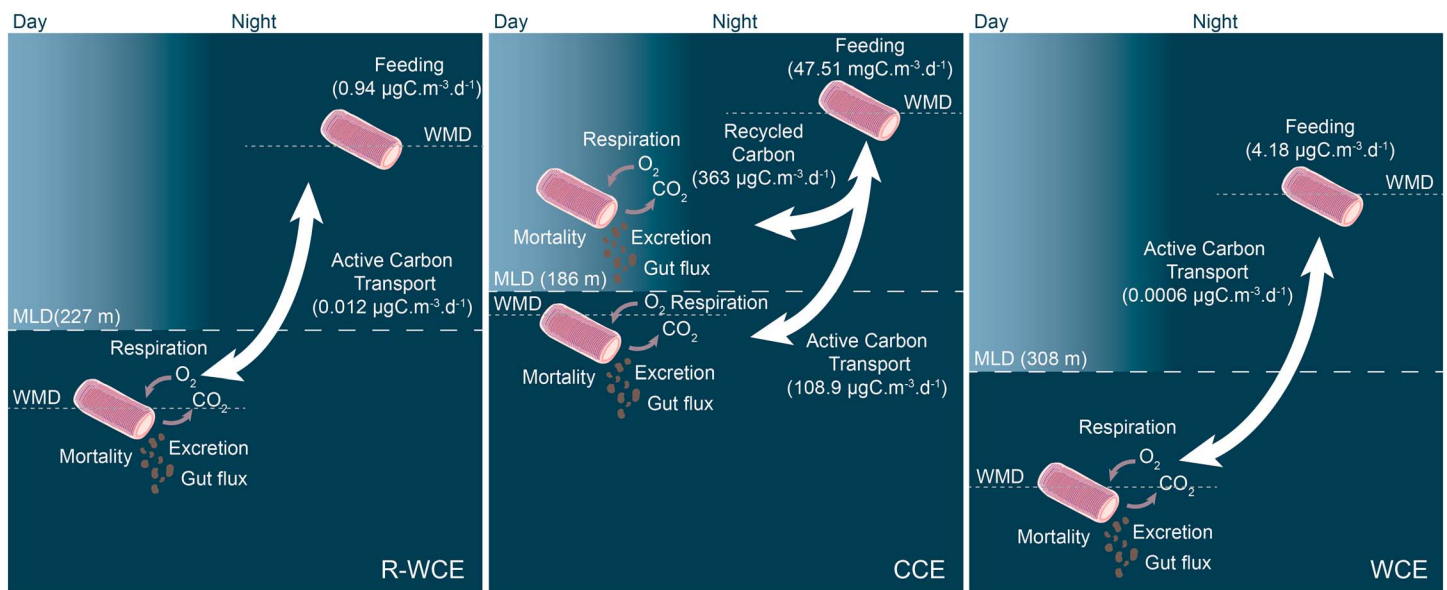
Figure 7. Conceptual diagram demonstrating *P. atlanticum* feeding, diel vertical migration, and contribution to active carbon transport in the R-WCE (left), CCE (middle), and WCE (right). The majority of active carbon transport in the CCE remained within the mixed layer (recycled carbon); however, 30% was transported below the mixed layer due to a bimodal daytime distribution of biomass (active carbon transport; see Figure 5). Photic zone depth in these eddies is unknown and is not necessarily synonymous with mixed layer depth. MLD = Mixed layer depth. WMD = Weighted mean depth; R-WCE = anti-cyclonic warm core eddy that formed from the retroflection of the East Australian Current; CCE = cold core eddy; WCE = warm core eddy.

downward active carbon flux by *Pyrosoma atlanticum* was estimated to be substantially higher in the CCE ($363 \ \mu g \ C \cdot m^{-3} \cdot d^{-1}$) than in the R-WCE ($0.02 \ \mu g \ C \cdot m^{-3} \cdot d^{-1}$) and the WCE ($0.04 \ \mu g \ C \cdot m^{-3} \cdot d^{-1}$). The contribution of each flux varied across water masses, with gut flux contributing the most to total downward carbon flux for the CCE (91%), and mortality contributing most to downward export in the R-WCE and the WCE (>99%; Table 3 and Figure 7).

4. Discussion

This study examined the vertical distribution and active carbon transport of *Pyrosoma atlanticum* across three eddies in the Tasman Sea in spring 2017. Pyrosome swarms have been observed previously in the Tasman Sea, but not quantified (Henschke et al., 2013; Thompson & Kesteven, 1942; Williams & Koslow, 1997). *P. atlanticum* were on average 2 orders of magnitude more abundant in the cold core eddy compared to the warm core eddies, reaching a maximum of 360 mg WW·m^{-3}, and to our knowledge the highest recorded biomass of *P. atlanticum* worldwide.

4.1. Respiration, Consumption, and Minimum Food Requirements

There are only two studies exploring the feeding dynamics of *Pyrosoma atlanticum* (Drits et al., 1992; Perissinotto et al., 2007), and this is the first study to calculate the respiration rate of *P. atlanticum*. Our respiration experiment demonstrated that the exponent (1.23; see equation (8)) was similar to values found

Table 3
Active Downward Carbon Flux for P. atlanticum From Nighttime Weighted Mean Depth (WMD) to Daytime WMD (See Figure 5)

Water mass	Respiratory flux ($\mu g \ C \cdot m^{-3} \cdot d^{-1}$)	Excretory flux ($\mu g \ C \cdot m^{-3} \cdot d^{-1}$)	Mortality flux ($\mu g \ C \cdot m^{-3} \cdot d^{-1}$)	Gut flux ($\mu g \ C \cdot m^{-3} \cdot d^{-1}$)	Total active carbon flux ($\mu g \ C \cdot m^{-3} \cdot d^{-1}$)
R-WCE	0.0002	0.00006	0.02	~0	0.02
CCE	0.12	0.037	30.8	331.5	362.5
WCE	0.0003	0.00009	0.04	0.000066	0.04

Note. Gut flux is corrected for time spent vertically migrating and is therefore corrected such that only the portion of food consumed in the surface waters during the night are considered a contribution to active carbon transport.

for salps (0.97–1.37) as well as other gelatinous zooplankton (0.88–1.15; Schneider, 1992). Correcting for temperature, respiration values from this study fit with previously determined respiration rates for other pelagic marine organisms (Figure 5c). Using previously established clearance rates (Drits et al., 1992; Perissinotto et al., 2007) and this study's respiration rate, we can determine the minimum food requirements for the three *P. atlanticum* populations.

Pyrosoma atlanticum populations in the CCE were estimated to be able to consume substantially more phytoplankton compared to the R-WCE and the WCE. In the CCE, estimated *P. atlanticum* consumption equated to 95% of the daily phytoplankton standing stock (47.51 mg C m^{-3}) while feeding at the surface, whereas in the R-WCE and CCE their impact on the phytoplankton stock was minimal, consuming much less than 1%. The high consumption in the CCE is proportionate to the biomass of pyrosomes (91% of total micronekton) and is comparable to swarms of other pelagic tunicates, such as salps, which have a grazing pressure that can exceed the daily primary production when abundant (Dubischar & Bathmann, 1997). Minimum food requirements across each eddy ranged from 10 to 24% of total daily consumption, suggesting that *P. atlanticum* colonies were able to allocate between 40 and 54% of daily consumption (i.e., the remainder minus egestion) to growth. Thus, they had potential growth rates of 0.6% body C d^{-1} in the CCE and 0.02–0.05% body C d^{-1} in the R-WCE and the WCE. There are no experimentally determined growth rates for pyrosomes; however, based on changes in weighted mean length, Andersen and Sardou (1994) estimated growth rates equivalent to ~30% body C d^{-1} for swarms occurring in high chlorophyll *a* conditions in the Ligurian Sea. This growth rate estimation is comparable to the fastest growth rates previously estimated experimentally for a similar sized salp (10–100 mm), *Cyclosalpa bakeri* (0.9–32% d^{-1}; Madin & Purcell, 1992), and several other salp species (Andersen & Sardou, 1994). Growth rates for salps tend to follow a von Bertalanffy curve, with the rate of growth declining with size (Madin & Deibel, 1998). *Pyrosoma atlanticum* colonies sampled by Andersen and Sardou (1994) were small (6–16 mm), whereas our CCE populations were larger (108 mm). Thus, it is likely that in optimal conditions, *P. atlanticum* growth rates can range from 30% body C d^{-1} when young to less than 1% body C d^{-1} as they reach maximum size. However, directly comparing growth rates between pyrosomes and salps may not be ideal as pyrosome colonies can increase in size by both the growth of individual zooids, or by the addition of new individual zooids (Sutherland et al., 2018), whereas as salp growth rates refer only to the increase in size of the individual. As it is difficult to accurately determine growth rates of gelatinous zooplankton from size-distributions in the field (due to their tendency to aggregate from physical turbulence; (Graham et al., 2001) experimental studies are necessary to validate these growth rates.

4.2. Active Carbon Transport

Although studies have speculated that pyrosomes are likely to contribute to downward active carbon flux (e.g., Sutherland et al., 2018), to our knowledge no studies have attempted to quantify *P. atlanticum* respiratory, excretory, mortality, or gut flux contribution to downward carbon transport. We found that the overall depth of DVM, and thus downward carbon flux, differed across water types. Within the R-WCE, CCE, and WCE, the proportion of pyrosome biomass vertically migrating into the mixed layer at night were 48%, 36%, and 66%, respectively.

Previous studies assessing downward flux of total zooplankton and micronekton communities in subtropical regions range from 0.6 to 107 mg C·m^{-2}·d^{-1} (Longhurst et al., 1990; Isla et al., 2015; see Supplementary Table S1 in Pakhomov et al., 2018). Although the entire population of *Pyrosoma atlanticum* migrated below the mixed layer during the day in the two WCEs, the R-WCE and the WCE, they were estimated to contribute relatively inconsequential amounts (2 and 4 µg C·m^{-2}·d^{-1}) to downward carbon flux, less than 1% of minimum values in this range. In the CCE, where *P. atlanticum* biomass was significantly greater, populations were estimated to produce 36.3 mg C·m^{-2}·d^{-1} (363 µg C·m^{-3}·d^{-1}) of active carbon. The vertical distribution of pyrosome biomass in the CCE was bimodal, with the majority of the population (70%) remaining within the mixed layer during the day and night and 30% of the population migrating below the mixed layer (Figure 7). Thus, it is likely that the majority of flux (70%) was being recycled within the mixed layer (Iversen et al., 2017), while only 30% was transported below the mixed layer between 300 and 500 m. This equates to an estimated downward carbon flux of 10.89 mg C·m^{-2}·d^{-1} (108.9 µg C·m^{-3}·d^{-1}), approximately 4 orders of magnitude greater than the flux transported in the R-WCE and the WCE (Figure 7), and within the range of observed fluxes for subtropical zooplankton and micronekton populations (Longhurst et al., 1990; Isla et al.,

2015; see Supplementary Table S1 in Pakhomov et al., 2018). Hence, pyrosomes play a substantial role in the active transport of carbon to depth, with a single species swarm capable of producing a flux that is equivalent to zooplankton and/or micronekton communities.

The relative contribution of each estimated flux to total downward export varied across water mass. In the R-WCE and the WCE, mortality contributed the most to downward carbon export, compared to gut flux in the CCE. Gut flux represents the nonassimilated food released via defecation and is generally thought to be greater for micronekton than zooplankton, due to their long gut passage times. For example, complete gut evacuation of zooplankton ranges from a few minutes to 90 min (e.g. Dam & Peterson, 1988; Gurney et al., 2002; Pakhomov et al., 2004), whereas micronekton fish gut evacuation can range from 18 hours to days in tropical/subtropical waters (Baird et al., 1975; Clarke, 1980). We applied a gut passage time of 1.43 hours for *P. atlanticum* (Perissinotto et al., 2007). As such, in the CCE and the WCE, our calculations suggest that pyrosomes were able to reach daytime residence depth prior to evacuating nondigested food consumed in the surface waters. As gut flux is proportional to individual size, it was a much greater proportion of active carbon transport in the CCE, where individuals were much larger, compared to the WCE. In the R-WCE time spent on downward migration exceeded gut passage time, suggesting that non-assimilated food was not successfully transported below the mixed layer by active migration. All other flux values were similar in the R-WCE and the WCE, which was expected as populations in the R-WCE and the WCE were of similar magnitude.

Assimilated carbon from nighttime surface feeding is transported to depth as energy stores, a portion of which is then released at depth via respiration in the form of dissolved inorganic carbon (DIC), and excretion in the form of DOC (Steinberg et al., 2000). The majority of active carbon transport studies to date focus on respiratory flux (Ariza et al., 2015) as relatively straightforward laboratory experiments can be conducted to quantify this flux for various species. In comparison, gut flux and mortality, which contribute to particulate organic carbon (POC) fluxes, are more difficult to quantify. While both are important components of the carbon cycle, POC generally is comprised of larger organic matter than DOC and DIC, which are comprised of molecules. Hence, POC will sink faster and contribute to passive carbon flux or can be repackaged into POC, DOC, or DIC through fragmentation, degradation, consumption, or respiration (Buesseler et al., 2008; Iversen et al., 2010; Iversen et al., 2017).

Downward active carbon flux is calculated based on the proportion of the community that is migrating. Here ~50% of total pyrosome biomass in each eddy were actively migrating. Due to difference between time spent migrating and gut passage times in the present study, we estimate ~3% of daily fecal pellet production (0.43 h) was transported below the mixed layer. Therefore, the relative proportions of fecal pellets being actively transported below the mixed layer in each eddy is minimal ($\lesssim$1.5%.) compared to the total daily fecal pellet flux produced by the whole (migrating and nonmigrating) pyrosome population. Similarly, the estimated mortality flux would only represent ~20% of total daily mortality. Thus, while the active downward carbon flux estimated for the *P. atlanticum* swarm in the CCE was comparable to other subtropical zooplankton and micronekton communities, it only represents a small proportion of the passive carbon flux potentially generated by the *P atlanticum* swarm.

4.3. Environmental Drivers of *Pyrosoma atlanticum* Swarms

The two warm core eddies, the R-WCE and the WCE, were characteristic of oligotrophic warm core eddies (Waite et al., 2007). They were deeply mixed with warm, saline water, and dominated by smaller (< 10 μm) phytoplankton. Micronekton and *Pyrosoma atlanticum* biomass were low, and *P. atlanticum* colonies were small, young and mostly reproductively immature. Alternatively, the CCE had significantly higher chlorophyll *a* concentrations and a greater proportion of larger phytoplankton cells (54%). In the CCE *P. atlanticum* biomass was 2 orders of magnitude greater, *P. atlanticum* colonies were larger and more mature compared to the warm core eddies, and the majority were of reproductive size.

Temperature has been assumed to be an important driver of *Pyrosoma atlanticum* swarms as they are commonly found in warmer regions (Andersen & Sardou, 1994; Drits et al., 1992; van Soest, 1981). However, *P. atlanticum* have been found in water as cool as 7 °C (Thompson, 1948), and high abundances have recently been observed in cool waters (~10 °C) of the northeast Pacific Ocean (Brodeur et al., 2018; Sutherland et al., 2018). In this study, *P. atlanticum* were exhibiting DVM with individuals sampled down to 800 m depth

(~7.6 °C), consistent with previous observations that have found *P. atlanticum* migrating down to 900 m depth (Andersen et al., 1992; Andersen & Sardou, 1994; Angel, 1989; Roe et al., 1987). *P. atlanticum* colonies migrating between 0 and 500 m would experience a temperature range of ~6 °C, and between 0 and 1,000 m a range of ~11 °C. Salps that migrate vertically have adaptations allowing them to be insensitive to changing temperatures due to the wide range in temperatures they would experience during descent/ascent (Harbison & Campenot, 1979), and it is likely that strong migrators like *P. atlanticum* would have a similar adaptation. There was no significant relationship between *P. atlanticum* biomass and temperature in our study, with populations occurring within their previously observed temperature ranges (16–20 °C). Instead, chlorophyll *a* concentration was a significant positive driver of *P. atlanticum* biomass; nighttime distributions of pyrosomes coincided with the local chlorophyll *a* maxima, and higher *P. atlanticum* biomass in the CCE occurred where phytoplankton cells were larger (>10 µm). While *P. atlanticum* are able to consume phytoplankton as small as 3 µm (Drits et al., 1992), *P. atlanticum* preferentially feed on particles >10 µm (Perissinotto et al., 2007). This suggests that the high biomass of *P. atlanticum* sampled in the CCE was likely a result of both increased chlorophyll *a* and the increased availability of preferred food. Comparable to other pelagic tunicates, our results suggest that *P. atlanticum* swarms are driven by food availability rather than temperature.

4.4. Concluding Remarks

Larger swarms of *Pyrosoma atlanticum* were observed in the CCE where there was increased proportions of preferred food to support the growing population. Colonies in this swarm were of reproductive size and growing faster than swarms in the warm core eddies, revealing that conditions within the CCE sustained the growth and development of such a large swarm. Across each eddy, *P. atlanticum* were estimated to be able to consume at least 3 times more food than their minimum food requirements, allowing for approximately half of consumption to be allocated to growth. This may explain why pyrosome swarms are able to rapidly develop and respond to favorable changes in environmental conditions. When abundant, *P. atlanticum* can consume 95% of phytoplankton carbon per day and may contribute substantially to downward carbon export. In the CCE migrating populations produced an estimated downward carbon flux that was 4 orders of magnitude greater than those in areas where pyrosome abundance was low, equivalent to fluxes for subtropical zooplankton and micronekton communities. Considering that pyrosome carcasses have a sinking rate of 1,300 m d^{-1} (Lebrato et al., 2013), the downward passive carbon flux (fecal pellets and carcasses) produced from these swarms are likely to be substantial.

References

Al-Mutairi, H., & Landry, M. R. (2001). Active export of carbon and nitrogen at station ALOHA by diel migrant zooplankton. *Deep Sea Research Part II: Topical Studies in Oceanography*, *48*(8-9), 2083–2103. https://doi.org/10.1016/S0967-0645(00)00174-0

Andersen, V., & Sardou, J. (1994). *Pyrosoma atlanticum* (Tunicata, Thaliacea): Diel migration and vertical distribution as a function of colony size. *Journal of Plankton Research*, *16*(4), 337–349. https://doi.org/10.1093/plankt/16.4.337

Andersen, V., Sardou, J., & Nival, P. (1992). The diel migrations and vertical distributions of zooplankton and micronekton in the north-western Mediterranean Sea. 2. Siphonophores, hydromedusae and pyrosomids. *Journal of Plankton Research*, *14*(8), 1155–1169. https://doi.org/10.1093/plankt/14.8.1155

Angel, M. V. (1989). Vertical profiles of pelagic communities in the vicinity of the Azores front and their implications to deep ocean ecology. *Progress in Oceanography*, *22*(1), 1–46. https://doi.org/10.1016/0079-6611(89)90009-8

Archer, S. K., Kahn, A. S., Leys, S. P., Norgard, T., Girgard, F., Du Preez, C., & Dunham, A. (2018). Pyrosome consumption by benthic organisms during blooms in the northeast Pacific and Gulf of Mexico. *Ecology*, *99*(4), 981–984. https://doi.org/10.1002/ecy.2097

Ariza, A., Garijo, J. C., Landeira, J. M., Bordes, F., & Hernández-León, S. (2015). Migrant biomass and respiratory carbon flux by zooplankton and micronekton in the subtropical Northeast Atlantic Ocean (Canary Islands). *Progress in Oceanography*, *134*, 330–342. https://doi.org/10.1016/j.pocean.2015.03.003

Baird, R. C., Hopkins, T. L., & Wilson, D. F. (1975). Diet and feeding chronology of *Diaphus taaningi* (Myctophidae) in the Cariaco Trench. *Copeia*, *1975*(2), 356–365. https://doi.org/10.2307/1442891

Berner, L. D. J. (1967). Distribution atlas of Thaliacea in the California current region. *Calcofi Atlas*, *8*, 1–322.

Bone, Q. (1998). Locomotion, locomotor muscles, and buoyancy. In Q. Bone (Ed.), *The biology of pelagic tunicates*, (pp. 35–53). New York: Oxford University Press.

Brodeur, R., Perry, I., Boldt, J., Flostrand, L., Galbraith, M., King, J., et al. (2018). *An unusual gelatinous plankton event in the NE Pacific: The great pyrosome bloom of 2017*, (Vol. *26*, pp. 22–27). Sidney, British Columbia, Canada: PICES Press.

Brodeur, R. D., Seki, M. P., Pakhomov, E. A., & Suntsov, A. V. (2004). *Micronekton—What are they and why are they important?* , (Vol. 13, pp. 7–11). Sidney, British Columbia, Canada: PICES Press.

Buesseler, K. O., Trull, T. W., Steinberg, D. K., Silver, M. W., Siegel, D. A., Saitoh, S. I., et al. (2008). VERTIGO (VERtical transport in the Global Ocean): A study of particle sources and flux attenuation in the North Pacific. *Deep Sea Research Part II: Topical Studies in Oceanography*, *55*(14-15), 1522–1539. https://doi.org/10.1016/j.dsr2.2008.04.024

Childerhouse, S., Dix, B., & Gales, N. (2001). Diet of New Zealand sea lions (*Phocarctos hookeri*) at the Auckland Islands. *Wildlife Research*, *28*(3), 291–298. https://doi.org/10.1071/WR00063

Clarke, T. R. (1980). Diets of fourteen species of vertically migrating mesopelagic fishes in Hawaiian waters. *Fisheries Bulletin*, *78*, 619–640.

Condie, S. A., & Dunn, J. R. (2006). Seasonal characteristics of the surface mixed layer in the Australasian region: Implications for primary production regimes and biogeography. *Marine and Freshwater Research*, *57*(6), 569–590. https://doi.org/10.1071/MF06009

Dam, H. G., & Peterson, W. T. (1988). The effect of temperature on the gut clearance rate constant of planktonic copepods. *Journal of Experimental Marine Biology and Ecology*, *123*(1), 1–14. https://doi.org/10.1016/0022-0981(88)90105-0

Drits, A. V., Arashkevich, E. G., & Semenova, T. N. (1992). *Pyrosoma atlanticum* (Tunicata, Thaliacea): Grazing impact on phytoplankton standing stock and role in organic carbon flux. *Journal of Plankton Research*, *14*(6), 799–809. https://doi.org/10.1093/plankt/14.6.799

Dubischar, C. D., & Bathmann, U. V. (1997). Grazing impact of copepods and salps on phytoplankton in the Atlantic sector of the Southern Ocean. *Deep-Sea Research Part II -Topical Studies in Oceanography*, *44*(1-2), 415–433. https://doi.org/10.1016/S0967-0645(96)00064-1

Everett, J. D., Baird, M. E., Oke, P. R., & Suthers, I. M. (2012). An avenue of eddies: Quantifying the biophysical properties of mesoscale eddies in the Tasman Sea. *Geophysical Research Letters*, *39*, L16608. https://doi.org/10.1029/2012GL053091

Gillooly, J., Brown, J., West, G., Savage, V., & Charnov, E. (2001). Effects of size and temperature on metabolic rate. *Science*, *293*(5538), 2248–2251. https://doi.org/10.1126/science.1061967

Godeaux, J. E. A., Bone, Q., & Braconnot, J. C. (1998). Anatomy of Thaliacea. In Q. Bone (Ed.), *The biology of pelagic tunicates*, (pp. 1–24). New York: Oxford University Press.

Graham, W. M., Pagès, F., & Hamner, W. M. (2001). A physical context for gelatinous zooplankton aggregations: A review. *Hydrobiologia*, *451*(1/3), 199–212. https://doi.org/10.1023/A:1011876004427

Gurney, L. J., Froneman, P. W., Pakhomov, E. A., & McQuaid, C. D. (2002). Diel feeding patterns and daily ration estimates of three subantarctic euphausiids in the vicinity of the Prince Edward islands (Southern Ocean). *Deep Sea Research Part II: Topical Studies in Oceanography*, *49*(16), 3207–3227. https://doi.org/10.1016/S0967-0645(02)00079-6

Harbison, G. R. (1998). The parasites and predators of Thaliacea. In Q. Bone (Ed.), *The biology of pelagic tunicates*, (pp. 187–214). New York: Oxford University Press.

Harbison, G. R., & Campenot, R. B. (1979). Effects of temperature on the swimming of salps (Tunicata, Thaliacea): Implications for vertical migration. *Limnology and Oceanography*, *24*(6), 1081–1091. https://doi.org/10.4319/lo.1979.24.6.1081

Hedd, A., & Gales, R. (2001). The diet of shy albatrosses (*Thalassarche cauta*) at Albatross Island, Tasmania. *Journal of Zoology*, *253*(1), 69–90. https://doi.org/10.1017/S0952836901000073

Henschke, N., Bowden, D. A., Everett, J. D., Holmes, S. P., Kloser, R. J., Lee, R. W., & Suthers, I. M. (2013). Salp-falls in the Tasman Sea: A major food input to deep sea benthos. *Marine Ecology Progress Series*, *491*, 165–175. https://doi.org/10.3354/meps10450

Henschke, N., Everett, J. D., Richardson, A. J., & Suthers, I. M. (2016). Rethinking the role of Salps in the ocean. *Trends in Ecology & Evolution*, *31*(9), 720–733. https://doi.org/10.1016/j.tree.2016.06.007

Henschke, N., Pakhomov, E. A., Groeneveld, J., & Meyer, B. (2018). Modelling the life cycle of Salpa thompsoni. *Ecological Modelling*, *387*, 17–26. https://doi.org/10.1016/j.ecolmodel.2018.08.017

Iguchi, N., & Ikeda, T. (2004). Metabolism and elemental composition of aggregate and solitary forms of *Salpa thompsoni* (Tunicata: Thaliacea) in waters off the Antarctic peninsula during austral summer 1999. *Journal of Plankton Research*, *26*(9), 1025–1037. https://doi.org/10.1093/plankt/fbh093

Isla, A., Scharek, R., & Latasa, M. (2015). Zooplankton diel vertical migration and contribution to deep active carbon flux in the NW Mediterranean. *Journal of Marine Systems*, *143*, 86–97. https://doi.org/10.1016/j.jmarsys.2014.10.017

Iversen, M. H., Nowald, N., Plough, H., Jackson, G. A., & Fischer, G. (2010). High resolution profiles of vertical particulate organic matter export off Cape Blanc, Mauritania: Degradation processes and ballasting effects. *Deep Sea Research Part I: Oceanographic Research Papers*, *57*(6), 771–784. https://doi.org/10.1016/j.dsr.2010.03.007

Iversen, M. H., Pakhomov, E. A., Hunt, B. P. V., van der Jagt, H., Wolf-Gladrow, D., & Klaas, C. (2017). Sinkers or floaters? Contribution from salp pellets to the export flux during a large bloom event in the Southern Ocean. *Deep Sea Research Part II: Topical Studies in Oceanography*, *138*, 116–125. https://doi.org/10.1016/j.dsr2.2016.12.004

Lebrato, M., de Jesus Mendes, P., Steinberg, D. K., Cartes, J. E., Jones, B. M., Birsa, L. B., et al. (2013). Jelly biomass sinking speed reveals a fast carbon export mechanism. *Limnology and Oceanography*, *58*(3), 1113–1122. https://doi.org/10.4319/lo.2013.58.3.1113

Lebrato, M., & Jones, D. O. B. (2009). Mass deposition event of *Pyrosoma atlanticum* carcasses off Ivory Coast (West Africa). *Limnology and Oceanography*, *54*(4), 1197–1209. https://doi.org/10.4319/lo.2009.54.4.1197

Longhurst, A. R., Bedo, A. W., Harrison, W. G., Head, E. J., & Sameoto, D. (1990). Vertical flux of respiratory carbon by oceanic diel migrant biota. *Deep Sea Research Part A: Oceanographic Research Papers*, *37*(4), 685–694. https://doi.org/10.1016/0198-0149(90)90098-G

Madin, L. P., & Deibel, D. (1998). Feeding and energetics of Thaliaceans. In Q. Bone (Ed.), *The biology of pelagic tunicates*, (pp. 43–64). New York: Oxford University Press.

Madin, L. P., & Purcell, J. E. (1992). Feeding, metabolism and growth of *Cyclosalpa bakeri* in the subarctic Pacific. *Limnology and Oceanography*, *37*(6), 1236–1251. https://doi.org/10.4319/lo.1992.37.6.1236

Marouchos, A., Underwood, M., Malan, J., Sherlock, M., & Kloser, R. J. (2017). *MIDOC: An improved open and closing net system for stratified sampling of mid-water biota*, (pp. 1–5). Aberdeen, UK: IEEE. https://doi.org/10.1109/OCEANSE.2017.8084931

Mayzaud, P., Boutoute, M., Gasparini, S., Mousseau, L., & Lefevre, D. (2005). Respiration in marine zooplankton—The other side of the coin: CO$_2$ production. *Limnology and Oceanography*, *50*(1), 291–298. https://doi.org/10.4319/lo.2005.50.1.0291

Montagnes, D. J. S., Berges, J. A., Harrison, P. J., & Taylor, F. J. R. (1994). Estimating carbon, nitrogen, protein, and chlorophyll-*a* from volume in marine phytoplankton. *Limnology and Oceanography*, *39*(5), 1044–1060. https://doi.org/10.4319/lo.1994.39.5.1044

Pakhomov, E. A., Atkinson, A., Meyer, B., Oettl, B., & Bathmann, U. (2004). Daily rations and growth of larval krill *Euphausia superba* in the eastern Bellinghausen Sea during austral autumn. *Deep Sea Research Part II: Topical Studies in Oceanography*, *51*(17-19), 2185–2198. https://doi.org/10.1016/j.dsr2.2004.08.003

Pakhomov, E. A., Podeswa, Y., Hunt, B. P. V., & Kwong, L. E. (2018). Vertical distribution and active carbon transport by pelagic decapods in the North Pacific subtropical gyre. *ICES Journal of Marine Science*. https://doi.org/10.1093/icesjms/fsy134

Perissinotto, R., Mayzaud, P., Nichols, P. D., & Labat, J. P. (2007). Grazing by *Pyrosoma atlanticum* (Tunicata, Thaliacea) in the South Indian Ocean. *Marine Ecology Progress Series*, *330*, 1–11. https://doi.org/10.3354/meps330001

Pitt, K. A., Duarte, C. M., Lucas, C. H., Sutherland, K. R., Condon, R. H., Mianzan, H., et al. (2013). Jellyfish body plans provide allometric advantages beyond low carbon content. *PLoS ONE*, *8*(8), e72683. https://doi.org/10.1371/journal.pone.0072683

Roe, H.S.J., Badcock, J., Billett, D.S.M., Chidgey, K.C., Domanski, P.A., Ellis, C.J., et al. (1987) Great Meteor East: A biological characterisation. Institiue of Oceanographic Sciences Deacon Laboratory. Report No. 248, 322 pp and microfiche

Schneider, G. (1992). A comparison of carbon-specific respiration rates in gelatinous and non-gelatinous zooplankton: A search for general rules in zooplankton metabolism. *Helgoländer Meeresuntersuchungen*, *46*(4), 377–388. https://doi.org/10.1007/BF02367205

Steele, J. H., & Henderson, E. W. (1993). The significance of interannual variability. In G. T. Evans, & M. J. R. Fasham (Eds.), *Towards a model of ocean biogeochemical processes*, (pp. 237–260). Berlin, Heidelberg: Springer Berlin Heidelberg. https://doi.org/10.1007/978-3-642-84602-1_12

Steinberg, D. K., Carlson, C. A., Bates, N. R., Goldthwait, S. A., Madin, L. P., & Michaels, A. F. (2000). Zooplankton vertical migration and the active transport of dissolved organic and inorganic carbon in the Sargasso Sea. *Deep Sea Research Part I: Oceanographic Research Papers*, *47*(1), 137–158. https://doi.org/10.1016/S0967-0637(99)00052-7

Strickland, J. D. H., & Parsons, T. R. (1972). *A practical handbook of seawater analysis*. Ottawa: Fisheries Research Board of Canada.

Sutherland, K. R., & Madin, L. P. (2010). Comparative jet wake structure and swimming performance of salps. *The Journal of Experimental Biology*, *213*(17), 2967–2975. https://doi.org/10.1242/jeb.041962

Sutherland, K. R., Sorensen, H. L., Blondheim, O. N., Brodeur, R. D., & Galloway, A. W. E. (2018). Range expansion of tropical pyrosomes in the Northeast Pacific Ocean. *Ecology*, *99*, 1–3.

Suthers, I.M. (2017) RV *Investigator* voyage summary: IN2017_V04. MNF, CSIRO. Accessed from: http://mnf.csiro.au/Voyages/Investigator-schedules/Plans-and-summaries/2017.aspx

Suthers, I. M., Young, J. W., Baird, M. E., Roughan, M., Everett, J. D., Brassington, G. B., et al. (2011). The strengthening east Australian current, its eddies and biological effects—An introduction and overview. *Deep Sea Research Part II: Topical Studies in Oceanography*, *58*(5), 538–546. https://doi.org/10.1016/j.dsr2.2010.09.029

Thompson, H. (1948). *Pelagic tunicates of Australia*. Melbourne: Commonwealth Council for Scientific and Industrial Research.

Thompson, H., & Kesteven, G. L. (1942). Pelagic tunicates in the plankton of south-eastern Australian waters, and their place in oceanographic studies. In *Bulletin*, (Vol. 153, pp. 151–156). Melbourne, Victoria, Australia: Council for Scientific and Industrial Research.

Tilburg, C. E., Subrahmanyam, B., & O'Brien, J. J. (2002). Ocean colour variability in the Tasman Sea. *Geophysical Research Letters*, *29*(10), 1487. https://doi.org/10.1029/2001GL014071

Uye, S., & Shimauchi, H. (2005). Population biomass, feeding, respiration and growth rates, and carbon budget of the scyphomedusa *Aurelia aurita* in the Inland Sea of Japan. *Journal of Plankton Research*, *27*(3), 237–248. https://doi.org/10.1093/plankt/fbh172

van Soest, R. W. M. (1981). A monograph of the order Pyrosomatida (Tunicata, Thaliacea). *Journal of Plankton Research*, *3*(4), 603–631. https://doi.org/10.1093/plankt/3.4.603

Waite, A. M., Pesant, S., Griffin, D. A., Thompson, P. A., & Holl, C. M. (2007). Oceanography, primary production and dissolved inorganic nitrogen uptake in two Leeuwin current eddies. *Deep Sea Research Part II: Topical Studies in Oceanography*, *54*(8-10), 981–1002. https://doi.org/10.1016/j.dsr2.2007.03.001

Williams, A., & Koslow, J. A. (1997). Species composition, biomass and vertical distribution of micronekton over the mid-slope region off southern Tasmania, Australia. *Marine Biology*, *130*(2), 259–276. https://doi.org/10.1007/s002270050246

Wood, S. N. (2006). *Generalized additive models: An introduction with R*. Boca Raton: Chapman & Hall/CRC. https://doi.org/10.1201/9781420010404